Zoomorphology (1992) 112:167–179

Zoomorphology

Morphology and morphometry of the lungs of two East African mole rats, *Tachyoryctes splendens* and *Heterocephalus glaber* (Mammalia, Rodentia)

J.N. Maina[1], G.M.O. Maloiy[2], and A.N. Makanya[1]

[1] Department of Veterinary Anatomy, University of Nairobi, P.O. Box 30197, Nairobi, Kenya
[2] Department of Zoology, Duke University, Durham, NC 27706, USA

Received March 10, 1991

Summary. The lungs of two fossorial rodents, the mole rat *Tachyoryctes splendens* and the naked mole rat *Heterocephalus glaber* were investigated by transmission and scanning electron microscopy and a comparative morphometric analysis of the lungs carried out in an attempt to find out whether there are any possible structural adaptational features which may be associated with fossoriality. The data from these two ecologically disparate fossorial rodents were compared with those of surface dwelling rodents on which equivalent data are available. Morphologically, the lung of *T. splendens* is essentially similar to that of terrestrial mammals while that of *H. glaber* shows features of underdevelopment. In *H. glaber*, a cuboidal epithelium extends down the respiratory tree to line what appear to be alveolar spaces, the blood capillaries constitute a double capillary system and the type I pneumocytes have microvilli on their free surface. Morphometrically, *H. glaber* has notably lower values indicative of rather unspecialized lungs. While the volume density of the parenchyma is 88% in *T. splendens*, that in *H. glaber* is only 76%. The blood-gas (tissue) barrier in *H. glaber* is notably thicker than in *T. splendens*. When normalized with body weight, the surface area of the blood-gas (tissue) barrier, the pulmonary capillary blood volume, the diffusing capacities of the tissue barrier and of the whole lung are consistently appreciably lower in *H. glaber*. When compared with *Mus musculus*, *Rattus rattus* and *Cavia porcellus*, *T. splendens* has somewhat comparable values with the surface dwelling rodents but the values of *H. glaber* are the lowest in the group. It is suggested that *T. splendens* has not undergone full adaptation to fossoriality as is supported by its behavioural activities, particularly those of occasionally surfacing to feed and making overland excursions. The low values of *H. glaber* may be commensurate with its extreme physiological adaptations for fossoriality, features which culminate in low basal metabolism and may in part explain paedomorphic traits of its respiratory system.

Correspondence to: J.N. Maina

A. Introduction

Among vertebrates, only a few taxa lead a fossorial mode of life and even among these, only a small number are known to conduct a completely subterranean existence. The strict requirements for this mode of life are evident in the notable evolutionary convergence both in the anatomy and physiology of the fossorial rodents (Eloff 1951). Animals inhabiting closed burrow systems are exposed to environments which are remarkably different from those above the surface. The microclimates of the burrows are more stable with respect to parameters such as temperature, light and humidity (Schmidt-Nielsen and Schmidt-Nielsen 1950; Mayer 1955; McNab 1966; Baudinette 1972; Gettinger 1975; Arieli 1979; Maclean 1981). The composition of gases in the burrows is considerably different from that of the normal atmosphere. Concentrations of carbon dioxide as high as 7–8% and of oxygen as low as 13–14% have been reported in burrows (Hayden 1966). The burrows of the pocket gopher (*Thomomys bottae* Wied, 1839) had a concentration of oxygen as low as 6% and carbon dioxide as high as 3.8% (McNab 1966; Darden 1970; Chapman and Bennet 1975). These atypical gaseous partial pressures are far beyond those which can be tolerated by surface-dwelling animals. Extreme hypoxia as well as hypercapnia affects cardiac function in most mammals (Faleschini and Whitten 1975; Tucker et al. 1976), induces artificial hypothermia and in some cases torpor (Chew et al. 1965; Bhattia et al. 1969; Hyden and Lindberg 1970; Studier and Proctor 1971), has a general depressing effect on growth (Thigpen 1940; Xu and Mortola 1989) and lowers the ventilation rate (Arieli and Ar 1979). The hypoxia that the mole rat (*Spalax ehrenbergi* Gueldenstaedt, 1770) can withstand is comparable to an altitude of more than 9000 meters (Arieli et al. 1977; Ar et al. 1977). Fossorial animals must have evolved structural and functional features which enable them to survive in the burrow conditions which are further characterized by perpetual darkness, high humidity and, in some cases, high temperatures. Due to a dearth of exten-

sive studies on the fossorial animals, the possibly diverse adaptations of burrow-dwelling animals "are only beginning to be understood" (Boggs et al. 1984). Studies on the structure of their lungs, which must significantly contribute towards survival in such habitats, are lacking.

The mole rat (*Tachyoryctes splendens* Rüppell, 1835) and the naked mole rat (*Heterocephalus glaber* Rüppell, 1842), which are the subjects of this study, are fossorial East African rodents which differ in body size, phylogenetic origin, behaviour and ecology. Aspects of the general biology of the naked mole-rat have recently been described in Sherman et al. (1991). The goals of the current study are: (1) to provide morphological details on the lungs of fossorial rodents, (2) to present a comparison of morphometric data on such species which lead similar modes of life but have adapted to remarkably different environmental demands, and (3) to compare pulmonary parameters between fossorial and non-fossorial rodents in an attempt to elucidate possible structural differences which may be associated with adaptation to fossoriality.

B. Materials and methods

Specimen collection. Four mature specimens of *T. splendens* and seven of *H. glaber* were investigated. The specimens of *T. splendens* were caught in Nairobi, an area with a mean annual temperature of 20° C, a mean annual rainfall of 650 mm, an altitude of 1800 m above sea level and the soil is a loose rich volcanic loam type. Specimens of *H. glaber* were caught in Tsavo National Park. The area is semi-arid, with a mean annual temperature of 27° C, a mean annual rainfall of less than 250 mm, an altitude of 900 m and the soil is extremely hard and stony. The specimens were caught by scooping them up after opening the burrow. In both cases, the specimens were killed, by an intraperitoneal injection of Euthatal® (20% pentobarbitone sodium), and weighed. The diaphragm was punctured on both sides of the mediastinum causing a pneumothorax and subsequent collapse of the lung. The trachea was cannulated and the lungs fixed by intratracheal instillation with 2.3% glutaraldehyde buffered in sodium phosphate (pH 7.2 and osmolarity 370 mosmol·l^{-1}) at a pressure head of 25 cm water with the animal in a supine position. When the fixative stopped flowing, a ligature was placed below the cannula. The lungs and the heart were carefully dissected out and a ligature placed at the tracheal bifurcation. The volume of the lung was determined by the weight displacement method (Scherle 1970).

Sampling. Grossly, the lungs of *T. splendens* and *H. glaber* are different. This necessitated different sampling procedures for the two species. In *T. splendens*, the left lung was cut into six transverse slices of equal thickness which were alternately processed for transmission electron microscopy (TEM) and light microscopy (LM). The lobes of the right lung were each cut into two equal transverse slices. One of the slices was used for TEM, the other for LM. In *H. glaber*, the sampling was essentially similar to that in *T. glaber*. The remaining tissues were set aside and processed for scanning electron microscopy (SEM).

Tissue processing. The slices for light microscopy were processed by standard techniques. Transverse (7 μm) thick sections were cut and stained with H&E. The first technically adequate section was used for the analysis of the parenchyma (the gas-exchange components of the lung) and the non-parenchyma (bronchi and blood vessels larger than capillaries). The slices for TEM were diced and processed through standard procedures; sections were cut from randomly picked blocks. A square lattice test system was printed onto the electron micrographs for analysis.

Scanning electron microscopy. Trachea and the lung samples were dehydrated in absolute alcohol, critical-point dried in liquid carbon dioxide and sputtered with gold palladium complex.

Morphometric analysis. The volume densities of the parenchyma (p) and the non-parenchyma (np) were determined by point-counting at a magnification of 100×. The ratio of the number of points on a component to those in the test system gives the volume density (V_v). Thus, for the parenchyma (p) the volume density is derived as:

$$V_{Vp} = Pp \cdot Pt^{-1} \quad (1)$$

The absolute volume of the parenchyma (Vp) is then calculated from the volume of the lung (VL). Thus,

$$Vp = V_{Vp} \cdot VL \quad (2)$$

The volume densities of the components of the parenchyma (the alveoli, blood capillaries and the interalveolar tissue) were determined by point counting. The volume density of the alveoli (V_{Va}) was arrived at as the ratio of points falling onto the alveolar lumina (Pa) and those in the whole test system (Pt). Thus,

$$V_{Va} = Pa \cdot Pt^{-1} \quad (3)$$

The absolute volumes were calculated from the volume of the parenchyma (Vp). Thus, for the alveoli the absolute volume (Va) was calculated as,

$$Va = V_{Va} \cdot Vp \quad (4)$$

The surface densities of the alveolar surface, the blood-gas (tissue) barrier, the capillary endothelium and the red blood cells were determined by intersection counting. The surface density of the alveoli (S_{Va}), for example, was calculated from the alveolar intersections (I) and the total length of the test system in real units (Lt), i.e. after correcting for the magnification. Thus,

$$S_{Va} = 2I \cdot Lt^{-1} \quad (5)$$

The surface areas were calculated from the densities and the volume of the parenchyma (Vp), the reference space. For the alveoli, the surface area (Sa) was calculated as follows:

$$Sa = S_{Va} \cdot Vp \quad (6)$$

The surface area of the plasma layer (Sp) was calculated as the average of the surface areas of the capillary endothelium (Se) and that of the red blood cells (Sr). Thus,

$$Sp = \frac{Se + Sr}{2} \quad (7)$$

The harmonic mean thickness of the blood-gas (tissue) barrier (τht) and that of the plasma layer (τhp) were determined by intercept length, measurement, using a linear scale. The τht was determined from the total number of intercepts (n), the sum of the reciprocals of the intercepts (Σ 1/L), and the final magnification (M). Thus,

$$\tau ht = \frac{(n)}{\Sigma\, 1/L} \cdot M^{-1} \quad (8)$$

Correction for possible overestimate in thickness due to obliqueness of sectioning was done by multiplying the harmonic mean values with correction factors of $\frac{2}{3}$ for τht and $\frac{3}{4}$ for τhp.

The arithmetic mean thickness (τt), which defines the quantity of the structural tissue of a barrier, was determined by point and intersection counting using a random (2 cm long) short-line grid as follows:

$$\tau t = \frac{z.p}{2.n} \cdot M^{-1} \quad (9)$$

where z is the length of the individual line, p the number of points on the barrier, n the number of intersections with the surfaces of the barrier and M the final magnification.

The diffusing capacity of a barrier or its conductance to a gas is directly proportional to surface area and inversely proportional

to thickness. It also depends on material properties of a barrier, a feature defined by a permeability coefficient (K). The diffusing capacities of the tissue barrier (Dto_2) and the plasma layer (Dpo_2) were calculated from the surface areas (S), the harmonic mean thickness (rh), and the physical constants for oxygen permeation (Ko_2). Thus, Dto_2 was determined as follows:

$$Dto_2 = Kto_2 \cdot \frac{(St)}{\tau ht} \tag{10}$$

where Kto_2 is the oxygen permeation coefficient through the tissue barrier, St the surface area of the tissue barrier and τht its harmonic mean thickness. The diffusing capacity of the plasma layer was in turn calculated from the surface area of the plasma layer, Sp (see Eq. 7), the harmonic mean thickness of the plasma layer (τhp) and the oxygen permeation coefficient through the plasma layer (Kpo_2). Thus,

$$Dpo_2 = Kpo_2 \cdot \frac{Sp}{\tau ht} \tag{11}$$

The diffusing capacity of the red blood cell (Deo_2) was determined from the pulmonary capillary blood volume (Vc) and the oxygen uptake coefficient by the whole blood (θo_2). Thus,

$$Deo_2 = Vc \cdot \theta o_2 \tag{12}$$

The membrane diffusing capacity (Dmo_2), the combined conductance of the tissue barrier (Dto_2) and the plasma layer (Dpo_2) was calculated as follows:

$$\frac{1}{Dmo_2} = \frac{1}{Dto_2} + \frac{1}{Dpo_2} \tag{13}$$

The total morphometric diffusing capacity of the lung (DLo_2) was in turn determined from the conductances of the three serial resistances which comprise the air-haemoglobin pathway namely Dto_2, Dpo_2 and Deo_2. Thus,

$$\frac{1}{DLo_2} = \frac{1}{Dto_2} + \frac{1}{Dpo_2} + \frac{1}{Deo_2} \tag{14}$$

The morphometric procedures used here are described in detail in Weibel (1979) and the model is essentially that outlined in Weibel (1970/71) and presented in Maina et al. (1989).

C. Results

I. Morphology

1. *Tachyoryctes splendens*

The trachea and the principal bronchi are lined by a pseudostratified columnar epithelium with ciliated (c) and goblet cells (g) (Figs. 1, 2). The columnar cells are arranged in distinct tracts on the epithelial surface and vary remarkably in height, presumably depending on the degree of elaboration of secretory materials. These cells occupy almost an equivalent epithelial surface area as the ciliated cells. The columnar cells have a spherical, centrally located nucleus and numerous diffuse electron-dense, intracytoplasmic secretory granules (Fig. 2, g). The epithelial cells are firmly attached to the basement membrane through an interlacing network of collagen fibres (arrows) and fibrocytes (arrowhead) and are joined together and to the basal cells across distinct junctional complexes (squares). The parenchyma (Fig. 3) mainly consists of rather hexagonal alveoli (arrows) with the respiratory bronchioles (arrowhead) being well developed. The non-parenchyma (non-respiratory blood and air conducting channels) consists of bronchi and blood vessels larger than capillaries (Fig. 3, v). Blood capillaries (ca) are intercalated in the interalveolar septum, protruding out into adjacent alveoli where the blood is well exposed to air on both sides (Figs. 4–6). The interalveolar septum is sporadically perforated (Fig. 4, arrow) by interalveolar pores. Supportive tissue elements such as collagen and elastic tissue are located in the thickest parts of the interalveolar septum (Fig. 6, square, triangle). It is possible that the thicker parts provide mechanical support while the thinner ones may serve as primary routes for gas exchange. Alveolar macrophages were frequently observed on the alveolar surface.

2. *Heterocephalus glaber*

The tracheal epithelium in *H. glaber* differs structurally in important details from that of *T. splendens*. The epithelium is predominantly composed of ciliated cells (c), with islets of lower cells (*n*) which are lined with microvilli (Fig. 7); columnar cells are relatively scarce. A cuboidal epithelium atypically extends as far down the respiratory tree as the alveolar duct and alveolar sac (Figs. 8, 9). The cells constituting this epithelium comprise ciliated columnar cells (c) (Fig. 8, arrowheads) and intercalated between them are basal cells (Fig. 8, s). The ciliated cells contain spherical, basally located nuclei and numerous mitochondria situated at the apical aspects of the cells. Secretory cells (n) contain diffuse mitochondria and spherical dense granules (Fig. 8). Such cells bear microvilli on the free surface; the epithelial cells are attached to a well-developed basement membrane (b) which contains (Fig. 9) fibrocytes, collagen (rhombs) and elastic tissue (squares).

The disposition of the blood capillaries along the interalveolar septum in *H. glaber* is uncharacteristic of all mammals that have been studied to a similar extent: the blood capillaries with erythrocytes (e) are largely located on opposite sides of the interalveolar septa (Fig. 10), the pulmonary capillary blood hence being effectively exposed to the alveolar (a) air only on one side (Fig. 11, inset). Further, the type I cells (ep) (squamous pneumocytes) bear microvilli on their free aspect (Fig. 11, arrowheads), a possible indication of incomplete differentiation of the alveolar pneumocytes. Alveolar macrophages are rarely observed on the alveolar surface.

II. Morphometry

1. *Tachyoryctes splendens*

The specimens which are of both sexes range in body mass from 126 to 256 g. Lung volume in turn ranges from 6 to 12 cm^3) (Table 1). In this species, the parenchyma comprises 88% of the lung while the non-parenchyma comprises only 12%. The parenchyma is made up of the alveoli (84%), blood capillaries (7%) and interal-

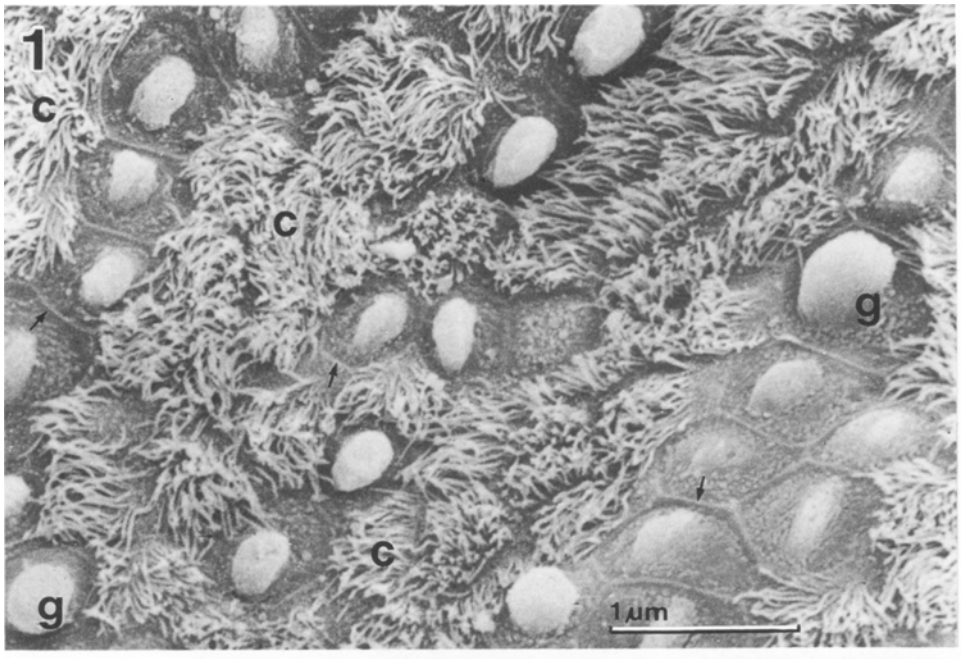

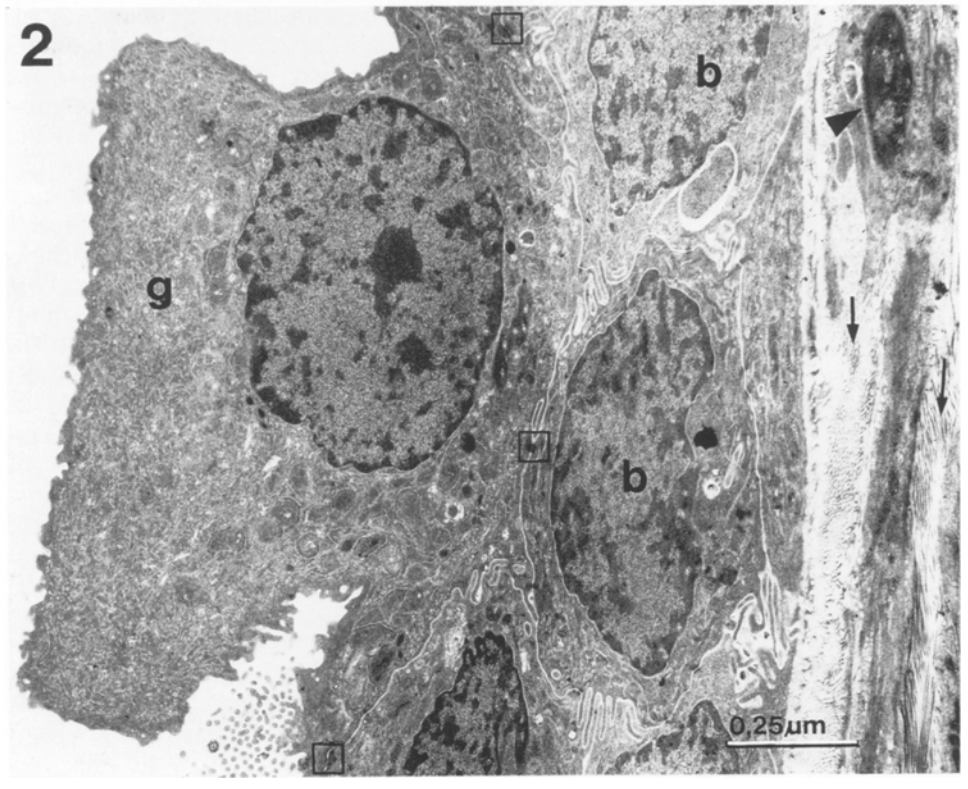

Fig. 1. Surface of the tracheal epithelium (SEM) of *Tachyoryctes splendens* showing numerous columnar cells (*g*) arranged in form of tracts, separated by ciliated cells (*c*). *Arrows* intercellular junctions

Fig. 2. Tracheal epithelium (TEM) of the tracheal epithelium of *T. splendens* showing a columnar (goblet) cell (*g*) overlying basal cells (*b*). Columnar cells, ciliated cells the basal cells fuse at distinct cell junctions (*squares*). Epithelial cells lie on a basement membrane consisting of collagen fibres (*arrows*) and fibrocytic cells (*arrowhead*)

veolar tissue (about 9%) (Table 2). In general, the alveolar surface area (Sa) exceeds that of the capillary endothelium (Sc) and also that of the red blood cells (Sr) (Table 3). The harmonic mean thickness of the blood-gas (tissue) barrier (τht) and that of the plasma layer (τhp) are 0.203 and 0.219 µm respectively. The arithmetic mean thickness (τt) is 0.678 µm.

The diffusing capacities of the components of the air-haemoglobin pathway are shown in Table 4. The diffusing capacity of the tissue barrier (Dto_2) is 0.0890 $mlO_2 \cdot sec^{-1} \cdot mbar^{-1}$ and that of the whole lung (DLo_2) is 0.0084 $mlO_2\ sec^{-1} \cdot mbar^{-1}$ (1 bar = 10^5 Pa).

2. *Heterocephalus glaber*

The specimens range in body mass from 23 to 43 g and the lung volume from 0.83 to 1.73 cm^3 (Table 1): according to the colonial size distribution suggested by Jarvis (1978), six out of the seven specimens which were captured are likely to have been workers while one (the

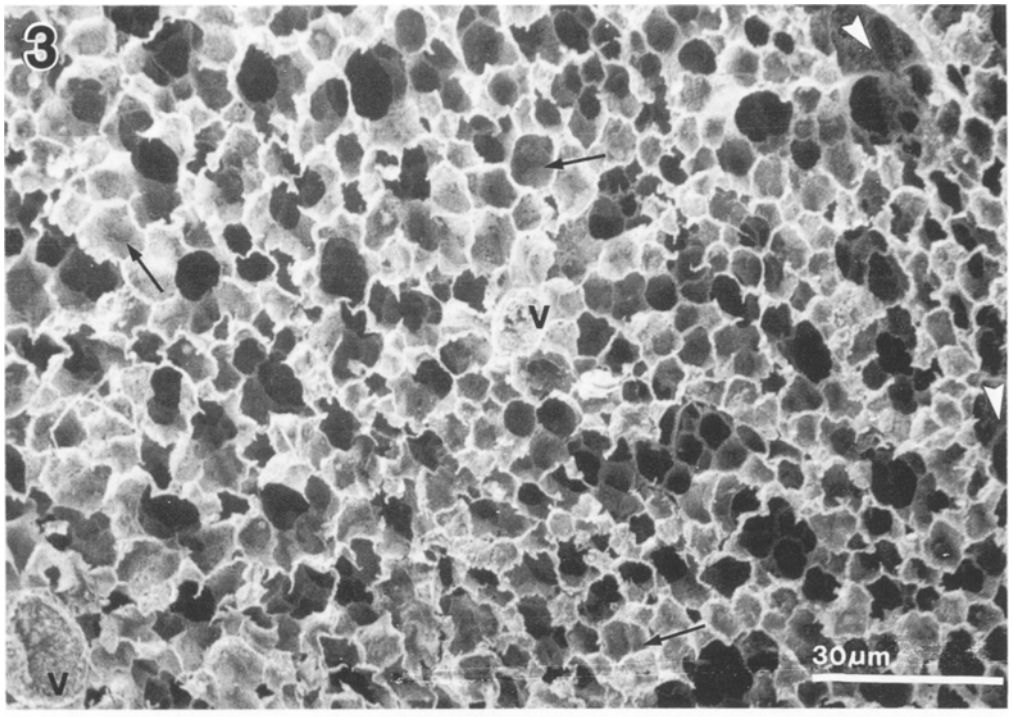

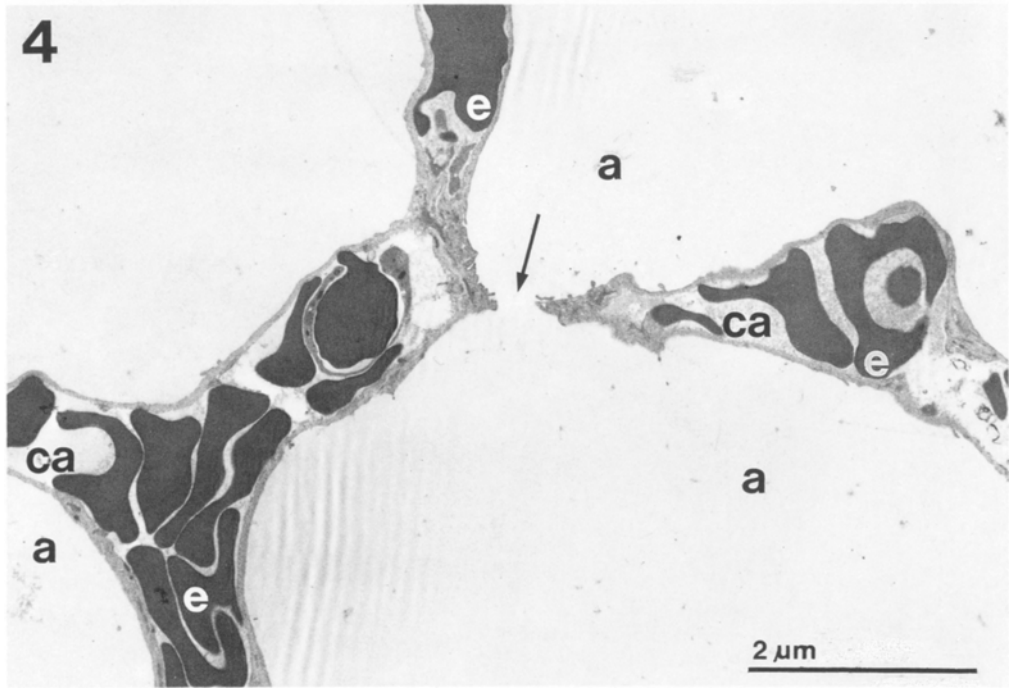

Fig. 3. Parenchyma of the lung (SEM) of *T. splendens* showing the alveoli (*arrows*) and large blood vessels (*v*). *Arrowheads* respiratory bronchioles

Fig. 4. Lung (TEM) of *T. splendens* showing alveoli (*a*) and the interalveolar septum containing blood capillaries and erythrocytes (*e*) contained in blood capillaries (*ca*). *Arrow* interalveolar pore

largest) was probably a non-worker. The volume density of the parenchyma was 76% and the non-parenchyma 24%. The parenchyma in turn is made up of alveoli (80%), blood capillaries (9%) and the interalveolar tissue about 11% (Table 2). The alveolar surface area (Sa) in general exceeds that of the capillary endothelium (Sc) and that of the red blood cells (Sr) (Table 3). Respectively, the harmonic mean thickness of the blood-gas (tissue) barrier (τht) and that of the plasma layer (τhp) are 0.243 and 0.210 µm (Table 3). The arithmetic mean thickness (τt) of the tissue barrier is 1.091 µm. The diffusing capacity of the tissue barrier (Dto_2) is 0.0132 $mlO_2 \cdot sec^{-1} \cdot mbar^{-1}$ and the total pulmonary diffusing capacity (DLo_2) 0.0012 $mlO_2 \cdot sec^{-1} \cdot mbar^{-1}$ (Table 4).

D. Discussion

I. Morphological comparison

Morphologically, the lungs of the mole rat (*T. splendens*) and the naked mole rat (*H. glaber*) differ structurally in some important details. In general, the structure of

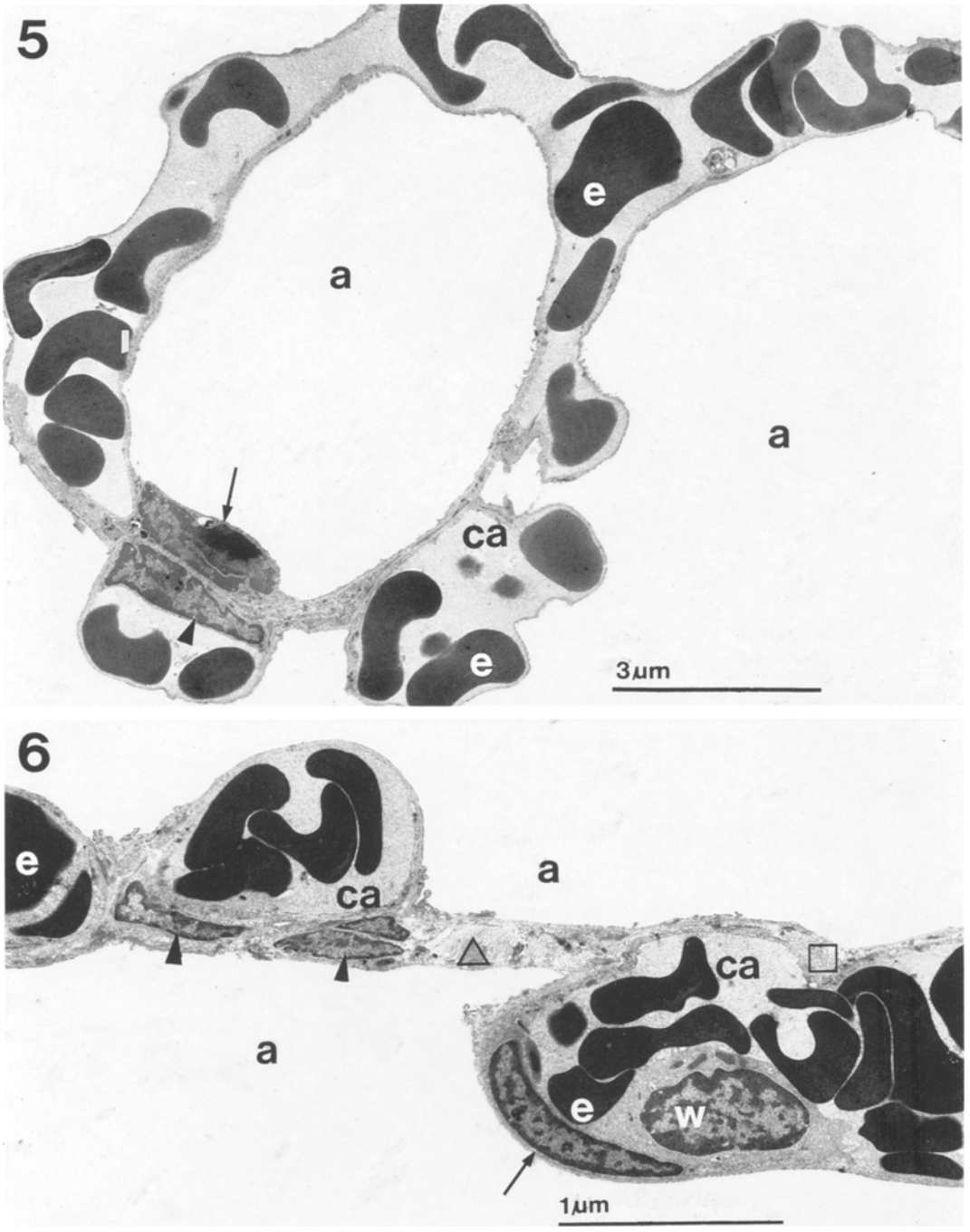

Fig. 5. Parenchyma (TEM) in the lung of *T. splendens* showing alveoli (*a*) and blood capillaries (*ca*) which contain red blood cells (*e*). *Arrow* type I [smooth] pneumocyte; *arrowhead* endothelial cell

Fig. 6. Interalveolar septum of the lung of *T. splendens* (TEM) showing the blood capillaries (*ca*) exposed to air on both sides. *a* alveoli; *e* erythrocyte; *w* white blood cell; *arrow* endothelial cell; *arrowheads* interstitial cells; *square* collagen; *triangle* elastic tissue. The supportive components of the lung (i.e. collagen and elastic tissue) are located on the thicker parts of the blood-gas (tissue) barrier where presumably very little if any gas exchange occurs

the lung of *T. splendens* is similar to that of a terrestrial (surface-dwelling) mammal (Weibel 1984). The same observations were made on the lung of the mole rat *Spalax ehrenbergi* by Arieli and Ar (1979). While the columnar cells are abundant in the tracheal and bronchiolar epithelium in *T. splendens*, these cells are very scarce in that of *H. glaber*. This feature may be due to the fact that in *H. glaber*, the elaborate tracheobronchiolar pseudostratified columnar epithelium gives way to a simple columnar and subsequently to a simple cuboidal ciliated epithelium which generally extends up to the levels of the alveolar ducts, sacs and what appear to be non-functional alveoli. Mucous secretory cells in *H. glaber* are scattered throughout the epithelial lining of the lung proximal to the alveolar surface. In virtually all the mammalian lungs that have been investigated so far,

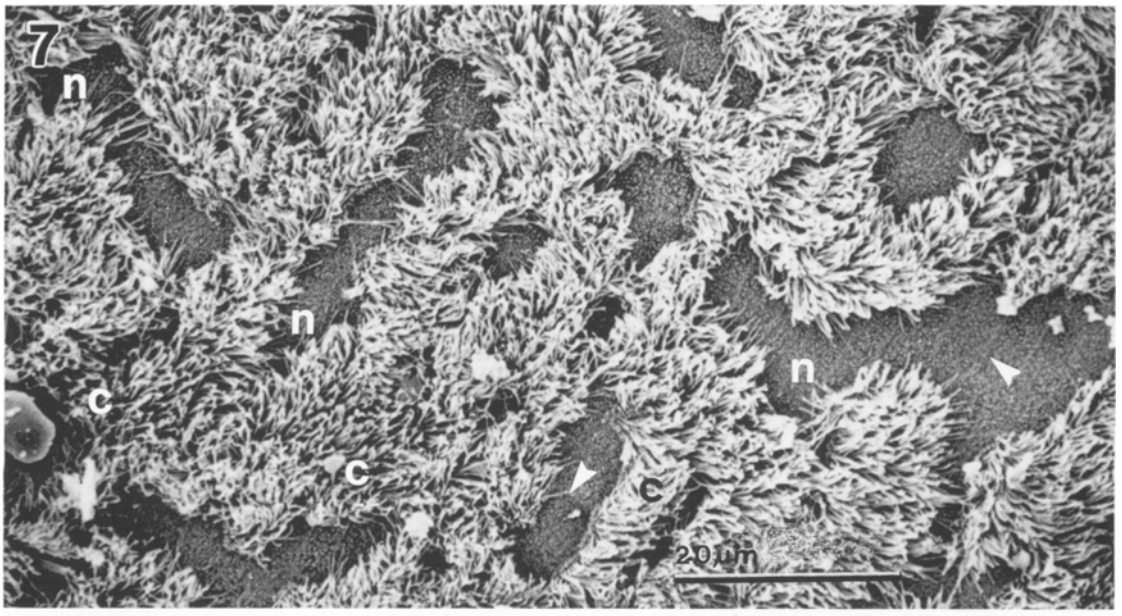

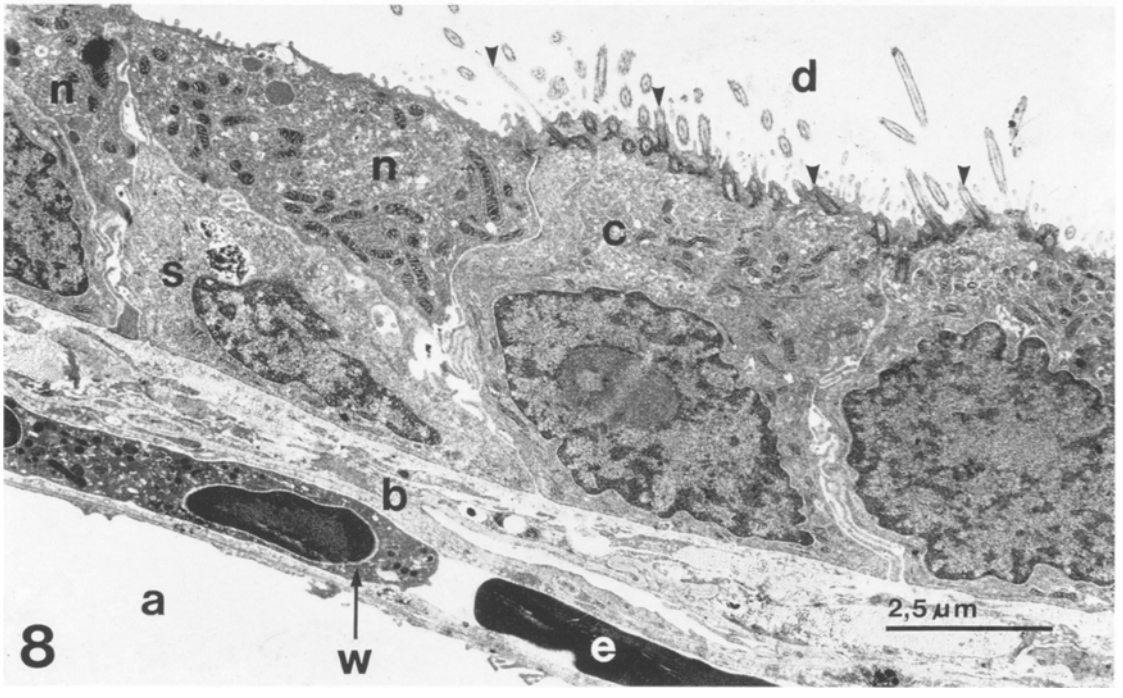

Fig. 7. Tracheal epithelium of *Heterocephalus glaber* (SEM) with ciliated cells (*c*) and nonciliated cells with microvilli (*n*). *Arrowheads* intercellular junctions. Note: columnar (goblet) cells were very scarce in this species much of the tracheal epithelium being covered by ciliated cells or nonciliated cells with microvilli (compare with Fig. 1 of *T. splendens*)

Fig. 8. Longitudinal section of cuboidal epithelium (TEM) in *H. glaber*; ciliated cells (*c*) and nonciliated cells (*n*) line an alveolar duct (*d*); alveolus (*a*) on adjacent side. Note: numerous mitochondria in both types of cells. *b* basement membrane; *e* erythrocyte; *w* white blood cells; *arrowheads* cilia; *s* basal cell

a simple ciliated columnar eithelium generally runs up to the terminal bronchiolar level (Breeze and Wheeldon 1975; Burri and Weibel 1977; Weibel 1984) where it gradually turns to a cuboidal one in the respiratory bronchiole and distally to a squamous epithelium which generally lines the alveolar duct, sac and alveolar surfaces. The distal continuity of the ciliated epithelium to the more dependent parts of the lung in *H. glaber* may account for the fact that alveolar macrophages were rarely observed in this species: these cells were seen in relatively greater frequency in the lung of *T. splendens*. It is plausible that the mucous escalator system in *H. glaber* starts much lower down the respiratory tree, a factor which may account for the dispensation with a large number of alveolar macrophages. Further, the extensive and elaborate epithelium may serve as a physical barrier to any invasive agents. Pulmonary tissue defence may be more critical in the burrow environment which contains a high concentration of dust [and possibly disease causing agents?]

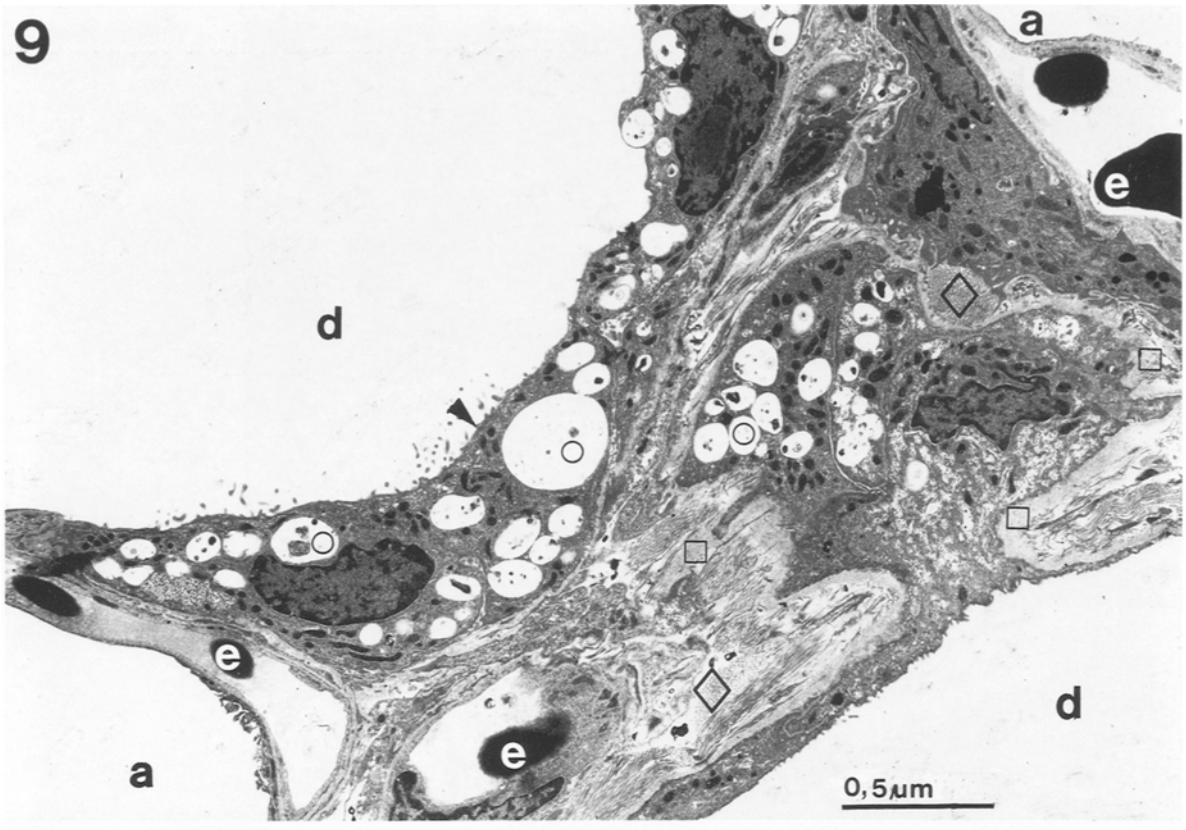

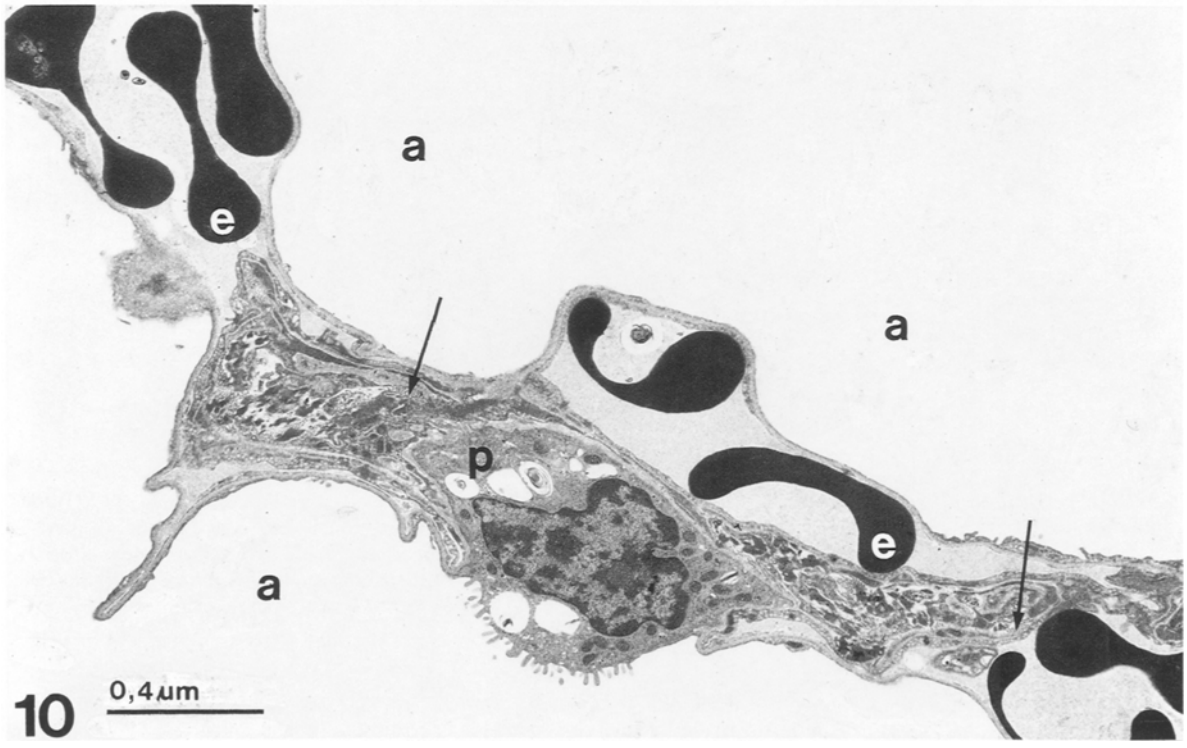

Fig. 9. Transverse section of parenchyma (TEM) of the lung of *H. glaber*, with cuboidal epithelium (*arrowhead*) lining an alveolar duct (*d*). *a* alveoli; *e* erythrocytes contained in the blood capillaries; *circles* vacuolated secretory granules of the epithelial cells; *rhombs* collagen fibres; *squares* elastic tissue

Fig. 10. Parenchyma of the lung (TEM) of *H. glaber*, with blood capillaries containing erythrocytes (*e*); some of the capillaries are exposed to air only on one side. *p* granular [type II] pneumocyte; *a* alveoli; *arrows* collagen in interalveolar septum

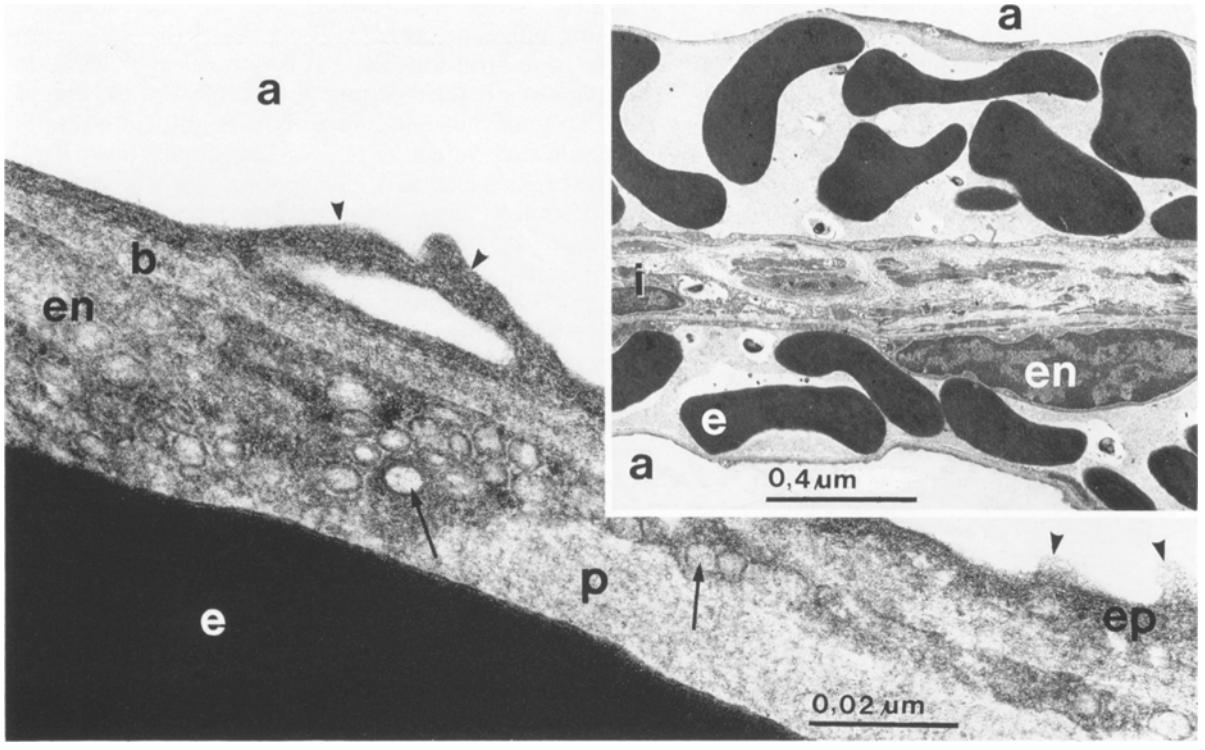

Fig. 11. Blood-gas (tissue) barrier of the lung (TEM) of *H. glaber*; endothelial cell (*en*) with micropinocytotic vesicles (*arrows*), an epithelial cell (*ep*) with microvilli (*arrowheads*) and basal lamina (*b*). *a* alveolus; *p* plasma; *e* erythrocyte. *Inset* shows area of the lung with blood capillaries located on opposite sides of the interalveolar septum constituting a double capillary system. *a* alveoli; *e* erythrocytes; *i* interstitial tissue and cells; *en* endothelial cell

Table 1. Body weight, lung volume, volume densities and absolute volumes of the parenchyma and the non-parenchyma of the lungs of the mole rats *Tachyoryctes splendens* and *Heterocephalus glaber*

Species/ specimen	Body weight	Lung volume	Parenchyma		Non-parenchyma	
	(g)	(cm^3)	(%)	(cm^3)	(%)	(cm^3)
Tachyoryctes						
1	255.49	11.55	89.5	10.34	10.5	1.21
2	199.20	7.35	84.2	6.19	15.8	1.16
3	125.60	7.38	87.2	4.92	10.6	0.58
4	197.00	7.38	87.2	6.44	12.8	0.94
Mean	194.32	7.95	87.58	6.97	12.43	0.97
SD (n±1)	53.21	2.56	2.49	2.34	2.49	0.29
Heterocephalus						
1	32	1.78	66.8	1.19	33.2	0.59
2	25	0.83	78.6	0.65	21.4	0.18
3	32	1.01	74.0	0.75	26.0	0.26
4	24	0.93	67.5	0.63	32.5	0.30
5	23	1.00	85.0	0.85	15.0	0.15
6	43	1.77	93.4	1.65	6.60	0.12
7	37	1.10	66.4	0.73	33.6	0.37
Mean	30.86	1.20	75.96	0.84	24.04	0.28
SD (n±1)	7.83	0.40	10.36	0.49	10.36	0.16

Table 2. Volume densities and absolute volumes of the components of the parenchyma namely alveoli, blood capillaries and interalveolar tissue in the lungs of the mole rats *T. splendens* and *H. glaber*. *Hc* pulmonary capillary haematocrit, the volume density of the red blood cells in the blood capillaries

Species/ specimen	Alveoli		Blood capillaries		Interalveolar tissue		Hc
	(%)	(cm^3)	(%)	(cm^3)	(%)	(cm^3)	(%)
Tachyoryctes							
1	86.42	8.94	6.84	0.71	6.74	0.70	59.26
2	84.08	5.21	6.49	0.40	9.43	0.54	59.85
3	82.86	4.08	6.08	0.30	11.06	0.54	74.00
4	81.79	5.27	10.88	0.70	7.32	0.47	62.3
Mean	83.78	5.88	7.57	0.53	8.64	0.57	63.99
SD (n±1)	1.99	2.12	2.23	0.21	1.99	0.10	66.86
Heterocephalus							
1	82.8	0.98	7.14	0.09	10.28	0.12	58.50
2	83.88	0.55	7.30	0.05	8.91	0.06	61.75
3	72.48	0.54	14.73	0.11	12.78	0.10	49.50
4	79.16	0.50	7.62	0.05	13.22	0.08	52.65
5	81.25	0.69	6.33	0.05	12.42	0.11	49.31
6	83.06	1.37	7.21	0.12	9.73	0.16	58.79
7	80.26	0.59	8.20	0.06	11.53	0.06	52.67
Mean	80.38	0.75	8.36	0.08	11.25	0.10	54.74
SD (n±1)	3.85	0.32	2.86	0.03	11.68	0.04	4.93

The arrangement of the blood capillaries on opposite sides of the interalveolar septa, constituting a double capillary system, as observed in *H. glaber* characterizes an early developmental stage of the mammalian lung (Burri 1974; Burri and Weibel 1977) and the "lower" vertebrate mature lungs (Meban 1980; Perry 1983; Maina 1987; Maina and Maloiy 1988). From the above observations, contrary to what has been pointed out by Thigpen (1940) on *H. glaber*, that "hypoxia has a depressing effect on growth" and that "the lung seems not to have been touched", it is quite clear that paedomorphosis, a feature defined as "shifting of the expression of some juvenile characteristics into adulthood" by Ayala and Valentine (1979), may typify most if not all the organ systems in this species. The differences in the inferences made here and those by Thigpen may be due to the fact that his interpretations were based on a histological investigation which could not possibly have provided adequate resolution for the fine structural features, compared to our observations. Although Weibel et al. (1980) pointed out that "respiration is too important a function for primitive features to be passed on in the structural organization of the respiratory system", the structure of the lung of *H. glaber* clearly does not appear to conform to this supposition, the principal features of underdevelopment being a double capillary system, a cuboidal epithelium that extends far down the respiratory pathways and undifferentiated alveolar pneumocytes.

Table 3. Surface areas of the alveoli (Sa), blood-gas (tissue) barrier (St), capillary endothelium (Sc) and the red blood cells (Sr) of the lungs of the mole rats *T. splendens* and *H. glaber*. Also shown are barrier thicknesses τht and τhp, respectively and harmonic mean thickness of the tissue barrier and the plasma layer. τt is the arithmetic mean thickness of the tissue barrier

Species/ specimen	Sa (m^2)	St (m^2)	Sc (m^2)	Sr (m^2)	τht (μm)	τhp (μm)	τt (μm)
Tachyoryctes							
1	1.248	0.882	0.924	0.699	0.177	0.212	0.500
2	0.814	0.468	0.508	0.357	0.230	0.219	0.733
3	0.719	0.392	0.419	0.350	0.251	0.187	0.808
4	0.794	0.672	0.726	0.732	0.153	0.257	0.670
Mean	0.894	0.604	0.644	0.535	0.203	0.219	0.678
SD (n±1)	0.240	0.220	0.227	0.209	0.045	0.029	0.131
Heterocephalus							
1	0.142	0.087	0.105	0.104	0.225	0.193	0.881
2	0.070	0.049	0.060	0.046	0.0264	0.207	0.878
3	0.095	0.071	0.100	0.097	0.258	0.252	0.764
4	0.083	0.051	0.064	0.052	0.221	0.196	1.000
5	0.105	0.070	0.090	0.061	0.250	0.209	1.400
6	0.192	0.119	0.140	0.126	0.244	0.185	1.735
7	0.093	0.060	0.070	0.243	0.211	0.229	0.982
Mean	0.111	0.072	0.090	0.077	0.243	0.210	1.091
SD (n±1)	0.042	0.024	0.028	0.031	0.020	0.023	0.348

II. Morphometric comparisons

Notable morphometric differences were observed between the lungs of *T. splendens* and those of *H. glaber*. The volume proportion of the parenchyma, i.e., the gas exchange region of the lung, in *T. splendens* is 88%, a value very close to the average value (85%) reported in terrestrial mammals by Gehr et al. (1981) whereas that of *H. glaber* is only 76%, the lowest value so far reported for a mammal. Despite these differences, the volume proportions of the components of the parenchyma are comparable, a feature which may suggest some general degree of optimization of the mammalian lung with respect to this parameter. The blood-gas (tissue)

Table 4. Diffusing capacities for oxygen through the blood-gas (tissue) barrier (Dto_2), plasma layer (Dpo_2), red blood cell (Deo_2), the membrane (Dmo_2) and the total morphometric pulmonary diffusing capacity (DLo_2) of the lungs of the mole rats *T. splendens* and *H. glaber*[a]. Units: $mlO_2 \cdot sec^{-1} \cdot mbar^{-1}$

	Dto_2	Dpo_2		Deo_2		Dmo_2		DLo_2	
		min.	max.	min.	max.	min.	max.	min.	max.
	0.0290	0.1530	0.2066	0.0080	0.0221	0.0244	0.0254	0.0060	0.0118
	0.0835	0.0788	0.1064	0.0045	0.0126	0.0405	0.0468	0.0041	0.0099
	0.0639	0.0823	0.1111	0.0034	0.0094	0.0360	0.0406	0.0031	0.0076
	0.0801	0.1136	0.1667	0.0079	0.0219	0.0697	0.0866	0.0071	0.0175
Mean±	0.0890	0.1070	0.1477	0.0060	0.0165	0.0427	0.0499	0.0051	0.0117
SD (n+1)	0.0650	0.0344	0.0479	0.0024	0.0065	0.0190	0.0261	0.0018	0.0042
	0.0159	0.0433	0.0585	0.0010	0.0027	0.0009	0.0125	0.0009	0.0022
	0.0076	0.0102	0.0137	0.0005	0.0015	0.0007	0.0007	0.0003	0.0005
	0.0110	0.0156	0.0210	0.0015	0.0034	0.0065	0.0072	0.0010	0.0023
	0.0094	0.0118	0.0159	0.0005	0.0015	0.0052	0.0059	0.0005	0.0012
	0.0115	0.0145	0.0196	0.0006	0.0017	0.0064	0.0073	0.0006	0.0014
	0.2000	0.0288	0.0388	0.0014	0.0037	0.0118	0.0132	0.0009	0.0029
	0.0181	0.0110	0.0148	0.0007	0.0019	0.0068	0.0082	0.0006	0.0015
Mean±	0.0132	0.0193	0.0260	0.0009	0.0023	0.0055	0.0079	0.0007	0.0017
SD (n+1)	0.0046	0.0123	0.0167	0.0004	0.0009	0.0038	0.0042	0.0003	0.0003

[a] The columns and rows showing the values of the individual species and specimens correspond with the positions shown in Tables 1 to 3 inclusive

Table 5. Normalized pulmonary morphometric parameters of the mole rats *T. splendens* and *H. glaber*. The parameters are further compared with those of other rodents on which comparable studies have been carried out. VL, lung volume; W, body weight; St, surface area of the blood-gas (tissue) barrier; Vp, volume of the parenchyma; vc, volume of the pulmonary capillary blood; τht, harmonic mean thickness of the tissue barrier; Dto_2, diffusing capacity of the tissue barrier; DLo_2, total pulmonary diffusing capacity

Parameter/ Units	*Tachyoryctes*	*Heterocephalus*	*Mus*	*Rattus*	*Cavia*
$VL \cdot W^{-1}$ ($cm^3 \cdot g^{-1}$)	0.04091	0.03918	0.03452	0.04529	0.03040
$St \cdot W^{-1}$ ($cm^2 \cdot g^{-1}$)	31.08	23.3	29.76	27.71	21.21
$St \cdot V \cdot p^{-1}$ ($mm^2 \cdot mm^{-3}$)	86.62	77.01	–	–	–
$Vc \cdot St^{-1}$ ($cm^3 \cdot m^{-2}$)	0.8775	1.056	1.1760	1.2371	1.6044
$Vc \cdot VL^{-1}$ ($cm^3 \cdot cm^{-3}$)	0.0667	0.0630	0.1014	0.0757	0.1100
$Vc \cdot W^{-1}$ ($cm^3 \cdot kg^{-1}$)	2.728	2.463	3.500	3.429	3.429
τht (μm)	0.2030	0.2430	0.2900	0.3700	0.4200
Dto_2 ($mlO_2 \cdot s^{-1} \cdot mbar^{-1} \cdot kg^{-1}$)	0.4580	0.4280	0.4280	0.3071	0.2070
$DLo_2 \cdot W^{-1}$ ($mlO_2 \cdot s^{-1} \cdot mbar^{-1} \cdot kg^{-1}$)	0.0432	0.0389	0.0507	0.0485	0.0417

Sources of data: *Tachyoryctes* and *heterocephalus*, this study; *Mus musculus* (Geelhaar and Weibel 1971); *Rattus rattus* (Burri and Weibel 1971); *Cavia porcellus* (Forrest and Weibel 1975)

barrier in *T. splendens* which is 0.203 μm thick (τht) is relatively thinner than that of *H. glaber* (0.243 μm): the overall thickness of the barrier with respect to the arithmetic mean thickness (τt) is 60% in *H. glaber*. When the various morphometric parameters are normalized with body mass, it was noted that *T. splendens* had a higher surface area of the blood-gas (tissue) barrier than *H. glaber*, higher pulmonary capillary blood volume ($Vc \cdot VL^{-1}$), better pulmonary capillary blood exposure to air, the capillary loading ($Vc \cdot St^{-1}$), higher diffusing capacity of the tissue barrier (Dto_2) and total anatomical pulmonary diffusing capacity (DLo_2) (Table 5). This indicates that *T. splendens* has a "superior" lung to *H. glaber*. Comparison with surface-dwelling rodents, e.g. the white mouse (*Mus musculus* Linné, 1758), the white rat (*Rattus rattus* Gray, 1821) and the guinea pig (*Cavia porcellus* Pallas, 1766), for which comparable data are available (Table 5), revealed that *H. glaber* in general has relatively low values while *T. splendens* has values generally similar to those of surface-dwelling rodents. The total morphometric diffusing capacity (DLo_2), the most comprehensive estimator of the structural capacity of the lung for gas exchange, in *H. glaber* (0.0389 $mlO_2 \cdot sec^{-1} \cdot mbar^{-1} \cdot kg^{-1}$) is the lowest among the five rodents being 30% lower than in the mouse (Geelhaar and Weibel 1971). A number of hypotheses can be offered to account for the pulmonary morphological and morphometric disparities between *T. splendens* and *H. glaber* and those between fossorial rodents and their surface-dwelling counterparts. From the few available studies, the differences appear to have occurred through a complex synergy of events which may be physiological, ecological, ethological and probably phylogenetic, as will briefly be outlined below.

III. Consideration of factors which may have influenced pulmonary design in T. splendens and H. glaber

1. Physiological factors

Various physiological adaptations associated with fossoriality have been reported in a number of subterranean dwellers. The principal ones are that fossorial animals have favourable haematological oxygen uptake and transport parameters (Hall 1965; Chapman and Bennet 1975; Ar et al. 1977; Kilgore and Birchard 1980), a tolerance to hypoxia (Arieli et al. 1977; Boggs et al. 1984), a relatively low body temperature and a generally low metabolic rate (McNab 1966; Arieli et al. 1977). *H. glaber* has a remarkably low body temperature which ranges from 30° to 32° C, a high thermal conductance and a very poor thermoregulatory ability (McNab 1966; Alexander 1991). Except for aestivating species, the infraeutherian mammals normally operate at a very narrow temperature range of 36° to 39° C. Yanav et al. (1989) showed that there is a direct correlation between body temperature and ambient temperature in *H. glaber*, making the species essentially poikilothermic and hence able to manage its energy budget more effectively. Even at its relatively small size, the metabolic rate of H. glaber is 40% lower than that expected of a mammal of similar size (McNab 1966). Oxygen consumption in *H. glaber* is 40–60% of the values predicted for the rodents of comparable size (McNab 1966). Lovegrove and Wissel (1988) demonstrated that a 36 g *H. glaber* has a similar mass-specific resting metabolic rate as a 1 kg Cape dune mole rat (*Bathyergus suillus* Illiger, 1811). *H. glaber* has a basal metabolic rate of only 0.66 $mlO_2 \cdot g^{-1} \cdot hr^{-1}$ while the sandrat (*Heliophobius argenteocinereus* Peters,

1846) and *T. splendens*, two East African fossorial rodents, respectively have values of 0.85 and 0.79 (McNab 1979). Due to the unusually high concentration of carbon dioxide in the burrows, it is likely that in *H. glaber*, the colony mates are most of the time adaptively in a state of hypercapnic torpor as has been reported in some rodents (Chew et al. 1965; Hyden and Lindberg 1970; Bhattia et al. 1969; Studier and Proctor 1971). While in general the basal metabolic rate in fossorial rodents is low, the value in *T. splendens* is only 84% of that expected from a terrestrial mammal of equivalent body mass, while the value for *H. glaber* may be as low as 40% (McNab 1966, 1988): oxygen consumption in *T. splendens* is 0.70 $mlO_2 \cdot g^{-1} \cdot hr^{-1}$ and that of *H. glaber* 0.55 $mlO_2 \cdot g^{-1} \cdot hr^{-1}$ (McNab 1966), a difference of about 30%. It is evident, from the available data, that while the metabolic demands of *T. splendens* are similar to those of terrestrial mammals (of similar size), *H. glaber* has relatively lower values. These features correspond with the observations made in this study that the lungs of *T. splendens* are morphologically and morphometrically adaptively similar to those of terrestrial mammals while *H. glaber* has "underdeveloped" and unspecialized lungs.

2. Ecological and ethological factors

The ecology and behaviour of *T. splendens* have been studied by Jarvis and Sale (1971). Their most pertinent findings were: compared with other East African mole rats such as *H. argenteocinereus* Peters, 1846, and *H. glaber*, *T. splendens* has the shortest burrow. It lives solitarily and prefers loose volcanic soils with higher moisture content. The lifestyle and some aspects of the morphology of *H. glaber* have been studied by Hill et al. (1957) and Jarvis (1978) with the following observations being relevant: *H. glaber* is the smallest of the Bathyergidae having an average body mass ranging from 20 to 34 g, it is entirely fossorial and is restricted to the arid regions of East Africa. It leads a colonial mode of life where as many as 295 mole rats have been reported to share a single burrow (Brett 1991). Though factors like soil texture, season, rain and microbial activity may influence burrow gas tensions (Arieli 1979), population density may be the primary determinant of this feature. So disparate are the ecological demands of *H. glaber* and *T. splendens* that sympatry does not occur between the two species (Jarvis 1984).

Turning to *T. splendens*, the species has a body temperature of 36° C which is reasonably within the mammalian range and the average burrow temperature of 23.2° C is very close to the atmospheric one. Its burrows are relatively shallow with an average depth of 0.15–0.25 m (McNab 1966). Though measurements of gas tensions in the burrows of *T. splendens* have not yet been made, it would be expected that with the porous volcanic soil it lives in, these parameters would differ very little, if at all, from the atmospheric ones. This species (Jarvis 1973; and from personal observations [J.N.M.]) comes occasionally to the surface at night to feed.

E. Conclusions

Phylogeny, physiological demands, mode of life and behaviour appear to have played a role (to yet unknown extents) in modulating the anatomy of the respiratory system of *H. glaber*. The species appears to have maintained and/or acquired relatively unspecialized lungs by essentially adopting distinct physiological and ethological stratagems which have culminated in remarkably reduced niche-energetic demands as reflected in its low basal metabolism. Nevertheless, the paedomorphic pulmonary characteristics of *H. glaber* may partly be conserved traits unique to its singular evolutionary history and may have been perpetuated by a lack of genetic diversity. It is, nonetheless, possible that *H. glaber* never reaches full organismal maturity until the last years of its relatively long and not well-known lifespan (Jarvis 1984). A slight possibility, however, exists that some of the specimens of *H. glaber* examined in this study could not have reached complete maturity and thus the observed features [in such specimens] may be developmentally transient. There is currently no accurate method of aging *H. glaber* except by body weight, a parameter which is variable and dependent on factors such as season, sexual dimorphism and the level of nutrition: according to Jarvis [personal communication to J.N.M.], a naked mole rat of over 30 g [as were four of our seven specimens] should safely be considered mature. More detailed studies are clearly essential to fully understand the causative factors, the derivation and the significance of these morphological features. As pointed out by Alexander (1991), "it is most unlikely that reasonable explanations for the unusual attributes of naked mole-rat will be developed without greater understading of its life-style and its evolutionary history". Unfortunately most of these details are at present unknown.

Acknowledgements. This work was supported by a generous grant from the Leverhulme Trust of London and was completed at the Department of Anatomy, School of Veterinary Medicine, University of California (Davis) when one of the authors (J.N.M.) was a Fulbright Senior Research Fellow. We wish to thank all those who have helped in the realization of this work. We are most grateful to the two editors and two anonymous reviewers.

References

Alexander RD (1991) Some unanswered questions about naked mole-rats. In: Sherman PW, Jarvis JUM, Alexander RD (eds) The biology of the naked mole-rat. Princeton University Press, Princeton, NJ, pp 446–465

Ar A, Arieli R, Shkolnik A (1977) Blood gas properties and function in the fossorial mole rat under normal and hypoxic-hypercapnic atmospheric conditions. Respir Physiol 30:201–218

Arieli R (1979) The atmospheric environment of the fossorial mole rat (*Spalax ehrenbergi*): effect of season, soil texture, rain, temperature, and activity. Comp Biochem Physiol 63A:569–575

Arieli R, Ar A (1979) Ventilation of a fossorial mammal *Spalax ehrenbergi* in hypoxic and hypercapnic conditions. J Appl Physiol 47:1011–1017

Arieli R, Ar A, Shkolnik A (1977) Metabolic responses of a fossorial rodent (*Spalax ehrenbergi*) to simulated burrow conditions. Physiol Zool 50:61–75

Ayala FJ, Valentine JW (1979) Evolving: The theory and the processes of organic evolution. Benjamin Cummings, Menlo Park, CA

Baudinette RV (1972) Energy metabolism and evaporative water loss in the California ground squirrel: effects of burrow temperature and water vapour pressure. J Comp Physiol 81:57–72

Bhattia B, George S, Rao TL (1969) Hypoxia and poilikothermia in rats. J Appl Physiol 27:583–586

Boggs DF, Kilgore DL, Birchard GF (1984) Respiratory physiology of burrowing mammals and birds. Comp Biochem Physiol 77A:1–7

Breeze RG, Wheeldon EB (1975) The cells of the pulmonary airways. Ann Rev Respir Dis 116:705–777

Brett RA (1991) The population structure of naked mole rat colonies. In: Sherman PW, Jarvis JUM, Alexander RD (eds) The Biology of the naked mole rat. Princeton (New Jersey), Princeton University Press, 97–136

Burri PH (1974) The postnatal growth of the rat lung. III. Morphology. Anat Rec 180:77–98

Burri PH, Weibel ER (1971) Morphometric estimation of pulmonary diffusion capacity. II. Effect pO_2 on the growing lung to hypoxia and hyperoxia. Respir Physiol 11:247–264

Burri PH, Weibel ER (1977) The ultrastructure and morphometry of the developing lung. In: Hodson WA (ed) Lung biology in health and disease: development of the lung. Mercel Dekker, New York, pp 215–268

Chapman RC, Bennet AF (1975) Physiological correlates of burrowing in rodents. Comp Biochem Physiol 51A:599–603

Chew R, Lindberg G, Hyden P (1965) Circadian rhythm of metabolic rate in pocket mice. J Mammal 46:477–494

Darden TR (1970) Respiratory adaptations of a fossorial mammal, the pocket gopher (*Thomomys bottae*). PhD dissertation, University of California (Davis)

Eloff G (1951) Adaptation in rodent moles and insectivorous moles and the theory of convergence. Nature (London) 168:1001–1002

Faleschini RJ, Whitten BK (1975) Comparative hypoxic tolerance in Sciuridae. Comp Biochem Physiol 52A:217–221

Forrest JB, Weibel ER (1975) Morphometric estimation of pulmonary diffusion capacity. IV. The normal guinea pig lung. Respir Physiol 24:191–202

Geelhaar A, Weibel ER (1971) Morphometric estimation of pulmonary diffusion capacity. III. The effect of increased oxygen consumption in Japanese waltzing mice. Respir Physiol 11:354–366

Gehr P, Mwangi DK, Amman A, Maloiy GMO, Taylor CR, Weibel ER (1981) Design of the mammalian respiratory system. IV. Scaling morphometric pulmonary diffusing capacity to body mass: wild and domestic mammals. Respir Physiol 44:61–86

Gettinger RD (1975) Metabolism and thermoregulation of a fossorial rodent, the northern pocket gopher (*Thomomys talpoides*). Physiol Zool 48:311–322

Hall FG (1965) Haemoglobin and oxygen affinities in seven species of Sciuridae. Science 148:1350–1351

Hayden JS (1966) Abnormal concentrations of respiratory gases in rabbit burrows. J Mammal 47:723

Hill OCW, Porter A, Bloom RT, Seago J, Southwick MD (1957) Field and laboratory studies on the naked mole rat *Heterocephalus glaber*. Proc Zool Soc (London) 128:455–514

Hyden P, Lindberg R (1970) Hypoxia induced torpor in pocket mice (genus Perognathus). Comp Biochem Physiol 33A:167–179

Jarvis JUM (1973) Activity patterns in the mole-rats *Tachyoryctes splendens* and *Heliophobius argenteocinereus*. Zool Afr 8:101–119

Jarvis JUM (1978) Energetics of survival in *Heterocephalus glaber* (Ruppell), the naked mole rat (Rodentia: Bathyergidae). In: Schlitter DA (ed) Bulletin of Carnegie Museum of Natural History (No. 6). Pittsburgh, Trustees of Carnegie Institute, pp 81–87

Jarvis JUM (1984) African mole rats. In: MacDonald D (ed) Encyclopedia of mammals, vol 2. London, Allen Unwin, pp 708–711

Jarvis JUM, Sale JB (1971) Burrowing and burrow patterns of East African mole rats *Tachyoryctes*, *Heliophobius* and *Heterocephalus*. J Zool (London) 163:451–475

Kilgore DL, Birchard GF (1980) Respiratory functions of blood in burrowing and nonburrowing birds. Am Zool 20:766–778

Lovegrove BG, Wissel C (1988) Sociality in mole rats: Metabolic scaling and the role of risk sensitivity. Oecologia (Berlin) 74:600–606

Maclean GS (1981) Factors influencing the composition of respiratory gases in mammal burrows. Comp Biochem Physiol 69A:373–380

Maina JN (1987) The morphology of the lung of the African lungfish (*Protopterus aethiopicus*): A scanning electron microscopic study. Cell Tissue Res 250:191–196

Maina JN, Maloiy GMO (1988) A scanning and transmission electron microscopic study of the lung of a caecilian *Boulengerula taitanus*. J Zool (London) 215:739–751

Maina JN, King AS, Settle G (1989) An allometric study of pulmonary parameters in birds, with mammalian comparisons. Phil Trans R Soc London B 326:1–57

Mayer WW (1955) The protective value of the burrow system to the hibernating Arctic ground squirrel (*Spermophilus tridecemlineatus*). Anat Rec 122:437–438

McNab B (1966) The metabolism of fossorial rodents: a study of convergence. Ecology 47:712–733

McNab B (1979) The influence of body size on the energetics and distribution of fossorial and burrowing mammals. Ecology 60:1010–1021

McNab B (1988) Complications inherent in scaling the basal metabolism in mammals. Quart Rev Biol 63:25–54

Meban C (1980) Thickness of the air-blood barrier in vertebrate lungs. J Anat 131:299–307

Perry SF (1983) Reptilian lungs: Functional anatomy and evolution. Adv Anat Embryol Cell Biol 79:1–81

Scherle WF (1970) A simple method for volumetry in organs in quantitative stereology. Mikroskopie 26:57–60

Schmidt-Nielsen B, Schmidt-Nielsen K (1950) Evaporative water loss in desert rodents in their natural habitat. Ecology 31:75–85

Sherman PW, Jarvis JUM, Alexander RD (1991) The biology of the naked mole-rat. Princeton (New Jersey), Princeton University Press

Studier EH, Proctor JW (1971) Respiratory gases in burrows of *Spermophilus tridecemlineatus*. J Mammal 52:631–633

Thigpen LW (1940) Histology of a normally hairless rodent. J Mammal 21:449–456

Tucker CE, James WE, Berry MA, Johnstone CJ, Glover RF (1976) Depressed myocardial function in the goat at high altitude. J Appl Physiol 41:356–361

Weibel ER (1970/71) Morphometric estimation of pulmonary diffusion capacity. I. Model and method. Respir Physiol 11:54–75

Weibel ER (1979) Stereological Methods: Practical methods for biological morphometry. London, Academic Press

Weibel ER (1984) The pathway for oxygen. Harvard University Press, Cambridge, MA

Weibel ER, Claassen H, Gehr P, Sehovic S, Burri P (1980) The respiratory system of the smallest mammal. In: Schmidt-Nielsen K, Bolis L, Taylor CR (eds) Comparative physiology of primitive mammals. Cambridge University Press, Cambridge

Xu L, Mortola JP (1989) Effects of hypoxia on the lung of the chick embryo. Can J Physiol Pharmacol 67:515–519

Yanav S, Buffenstein R, Jarvis JUM, Mitchell D (1989) Thermoregulation and evaporative water loss in the naked mole-rat, *Heterocephalus glaber*. S Afr J Sci 85:340